JOURNAL OF AGRICULTURAL AND FOOD CHEMISTRY
ARTICLE

J. Agric. Food Chem. 2009, 57, 5121–5128 5121
DOI:10.1021/jf803707a

FT-IR Methodology for Quality Control of Arabinogalactan Protein (AGP) Extracted from Green Tea (*Camellia sinensis*)

Xiao-Ling Zhou,[†,§] Ping-Nan Sun,[†,§] Peter Bucheli,[‡] Tian-Hua Huang,*[,†] and Dongfeng Wang[#]

[†]Shantou University Medical College, 22 Xinling Road, Shantou 515041 Guangdong, China, [‡]Science and Research, Building E-F, Nestlé R&D Center Beijing Ltd., No. 5 DiJin Road, Haidian District, Beijing 100095, China, and [#]College of Food Science, Ocean University of China, Qingdao 266003, China, [§]Co-first authors

A rapid methodology of quality control was developed for arabinogalactan proteins (AGP) extracted and purified from green tea. Using the vectorial angle method and IR spectrum analysis, the 1200−800 cm^{-1} region in second-derivative IR spectra was determined as the key fingerprinting region of green tea AGP, with the 1090−900 cm^{-1} region reflecting their conservative and common characteristics. In fact, the key monosaccharides, galactose (Gal) and arabinose (Ara), were shown to have intense peaks at about 1075 and 1045 cm^{-1}, respectively, and uronic acids at about 1018 cm^{-1} in second-derivative IR spectra. The variable region was identified to be at about 1134−1094 and 900−819 cm^{-1} and was probably due to compositional and structural differences between AGPs. The constructed methodology was tested on green tea AGP extracted by three treatments and purified to apparent homogeneity as water-extracted *Camellia sinensis* AGP (CSW-AGP), pectinase-extracted *C. sinensis* AGP (CSP-AGP), and trypsin-extracted *C. sinensis* AGP (CST-AGP) with an Ara/Gal ratio of 1.37, 1.57, and 1.82, respectively. Regarding in vitro antioxidant activity, the AGPs (CSW-AGP and CST-AGP) with higher similarity (closer cos θ values calculated for second-derivative IR spectra) exhibited a similar ability of chelating ferrous ions and had a similar capability for scavenging hydroxyl radicals. In conclusion, the combination of second-derivative IR spectrum analysis and the vectorial angle method has allowed a successful characterization of green tea AGPs and was shown to be suitable for their compositional and activity discrimination and rapid quality evaluation.

KEYWORDS: Rapid evaluation; quality control; arabinogalactan protein (AGP); green tea; FT-IR; second-derivative IR; antioxidant activity

INTRODUCTION

Plant arabinogalactans (AG) alone or associated with proteins (AGP), which play an important role in vegetative, reproductive, and cellular growth and development as well as programmed cell death, were shown to be potential immunological regulators for human health (*1*−*5*). Recently, Cipriani described an AG from *Maytenus ilicifolia*, consisting of arabinose, galactose, galacturonic acid, 4-*O*-methylglucuronic acid, rhamnose, and glucose in a 42:41:6:5:4:2 molar ratio, which could significantly inhibit ethanol-induced gastric lesions in rats and had a protective antiulcer effect (*6*). In another recent study Burgalassi revealed that larch AG might be a potential therapeutic product for dry eye protection and for the treatment of corneal wounds (*7*).

AG are frequently incorporated into foods as a soluble and nonviscous dietary fiber. They readily absorb in water and can be added to beverages in high concentrations without changing the taste, mouthfeel, or viscosity. AG are also used as an aid for suspending flavorings and colorings with low viscosity and for slowing the hardening process in the manufacture of hard candy (*8*). The combination of their physicochemical properties and potential health benefits makes AG and AGPs ideal candidates for food and medical applications.

Control of quality is critical in the use of polysaccharides in general as their physicochemical properties or bioactivities may change with the manufacturing process or the raw material origin and composition as well as the molecular distribution. Frequently, total sugar content is used as an index to control the content and quality of polysaccharide extracts. However, total sugar determination has great limitations for it can reflect neither the compositional variations nor the relationship of bioactivities and compositional or structural variations. The use of fingerprinting of macromolecules may overcome these limitations.

A lot of studies were published on the fingerprinting of macromolecules such as starch, cellulose (*9*), pectins (*10*), hemicelluloses, arabinoxylans (*11*), and polysaccharides from Lingzhi (*12*), but so far, the analytical characterization of AGP was not

*Address correspondence to this author (telephone +86 754 88900845; fax +86 754 88900845; e-mail xiaolingsmiling@yahoo.com.cn).

 Published on Web 05/20/2009

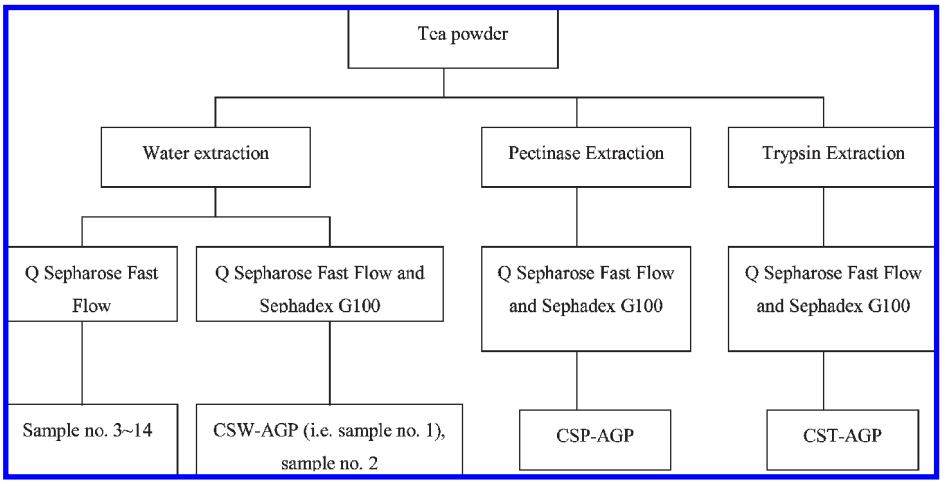

Figure 1. Samples obtained from tea powder.

really considered as a fingerprinting tool for use on AGPs extracted from green tea leaves. Performing IR and antioxidant activity measurement on the AGPs extracted from green tea, we demonstrated in this study that a combination of vectorial angle method and IR analysis can be used for the rapid discrimination and quality evaluation of AGPs obtained from different extraction treatments and that this approach can be effective for their fingerprinting.

MATERIALS AND METHODS

Materials and Chemicals. Leaves of green tea were collected from a tea market (Shantou, China) and were air- and oven-dried at 45 °C until the weight was constant. Monosaccharides, dextran, and chitosan were purchased from Sigma-Aldrich (Shanghai, China). Commercial crude tea polysaccharides samples 15 and 16 were purchased from Hainan Groupforce Pharmaceutical Co., Ltd.; samples 17 and 18 were purchased from Wuxi Green Power Bioproduct Co., Ltd. Pectinase (>1 unit/mg) was purchased from Sigma-Aldrich. Trypsin (>2500 units/mg) was purchased from Amresco (Solon, OH). Other chemicals were bought from China Pharm Chemicals Co. Ltd. (Shanghai, China).

Sample Preparation (Figure 1). Dried leaves of green tea were pulverized into powder that was treated with 80% ethanol to remove most of the pigment and oven-dried at 45 °C. Three processes were used to extract AGP from the decolored powder. In the first process, the powder was stirred in water (1:20, w/v) at 75 °C. In the second process, the powder was stirred in citric acid/sodium citrate buffer (1:20, w/v) (pH 3.0, 0.1 M) at 50 °C with 0.1% pectinase. In the third process, the powder was stirred in Na_2HPO_4/citric acid buffer (1:20, w/v) (pH 8.0, 0.2 M) at 37 °C with 0.1% trypsin. After 1 h of reaction, each extract was filtered, and the filtrate was centrifuged at 400*g* for 10 min. The obtained supernatant was freeze-dried and used to separate and purify AGP according to the procedures described previously for tea polysaccharide fraction (TPF) (*13*). Basically, AGPs were partially purified on a Q Sepharose Fast Flow column (20 mm × 60 cm) by a NaCl gradient at pH 8.0. Among the two fractions obtained, the second polysaccharide fraction was collected and further purified on a Sephadex G100 column (16 mm × 60 cm). The main polysaccharide fraction was collected and freeze-dried.

High-Performance Gel Permeation Chromatography (HPGPC) and Composition Analysis of the Extracted AGPs. The molecular mass distributions of CSW-AGP, CSP-AGP, and CST-AGP were determined by HPGPC using a TSK3000 column (7.8 mm × 30.0 cm, Tosoh Biosciences) that was eluted isocratically with ddH_2O at 35 °C with a flow rate of 0.5 mL/min, and using UV absorption and refractive index detectors. Standard dextrans T-10, T-40, T-70, T-110, and T-500 and blue dextran (Pharmacia) were used for the molecular size calibration. The monosaccharide analysis of the three AGPs was conducted according to Endwin's method (*14*) on an Agilent GC 6850 using a DB225 capillary column (30 m × 0.32 mm × 25 μm), with a gas velocity of 1 mL/min, FID detect, and a column temperature of 220 °C. The AGPs (25 mg) were dissolved in 6 M HCl and hydrolyzed in sealed evacuated tubes at 110 °C for 20 h and the respective products of hydrolysis were assayed in an Hitachi 835-50 amino acid analyzer. The uronic acid content in AGPs was determined according to the method of Blumenkrantz (*15*) and protein according to the Bradford method (*16*).

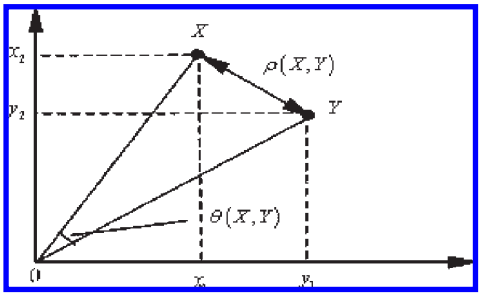

Figure 2. Vectorial angle method displayed by calculation of the similarity between two-dimension vectors of *X* and *Y*.

Fourier Transform Infrared Spectroscopy. The samples were kept at 40 °C until the weight was constant, and 2 mg was incorporated into 200 mg of KBr (spectroscopic grade) and pressed into a 1 mm pellet. The infrared spectra were collected on a Nicolet NEXUE470 spectrometer equipped with a DTGS detector. They were recorded in the transmission mode from the accumulation of 32 scans in the 1200−800 cm^{-1} range with a resolution of 4 cm^{-1}. The absorbance and first- and second-derivative IR spectra were obtained using OMNIC ESP V6 software.

Assessing the Similarity between the Spectra of the Extracted AGPs. The vectorial angle method (**Figure 2**) was used for evaluating the similarity between two spectral fingerprints. A spectrogram can be treated as a vector of hyperspace, and the similarity between them can be determined according to a vectorial angle formula (*17*−*19*).

$$\cos\theta = \frac{XY}{|X||Y|} = \frac{\sum_{i=1}^{n} x_i y_i}{\sqrt{\sum_{i=1}^{n} x_i^2 \sum_{i-1}^{n} y_i^2}}$$

Each specific spectrogram can be taken as a vector that is composed of a series of absorbance values corresponding to each wavenumber. *X* is the vector composed of a series of absorbance values corresponding to *n* wavenumbers ($x_1, x_2, x_3, ..., x_n$); *Y* is another vector composed of a series of absorbance values corresponding to *n* wavenumbers ($y_1, y_2, y_3, ..., y_n$); the inner product of vectors *X* and *Y* is $XY = x_1y_1 + x_2y_2 + x_3y_3 + ... + x_ny_n$, module of vector *X* is $|X| = (x_1^2 + x_2^2 + x_3^2 + ... + x_n^2)^{1/2}$, modules of vector *Y* is $Y| = (y_1^2 + y_2^2 + y_3^2 + ... + y_n^2)^{1/2}$. The closer to 1 the value of cos θ is, the more similar are the vectors *X* and *Y*. In this study, a program designed by Dr. Pingnan Sun was used in calculating the similarity of two spectrograms.

Table 1. Components of AGP Extracted from Tea[a]

component	sample															
	1 (CSW-AGP)	2	3	4	5	6	7	8	9	10	11	12	13	14	CSP-AGP	CST-AGP
Rha (mol %)	5.8	4.4	5.7	4.7	6.5	4.0	7.7	3.5	6.6	5.9	3.7	5.8	17.9	19.3	10.5	4.8
Fuc (mol %)				16.0		2.1		0.9		0.9			1.8			
Ara (mol %)	55.3	61.2	37.2	33.8	42.0	38.3	41.9	33.1	40.7	39.7	32.6	33.0	25.1	27.0	50.3	58.5
Xyl (mol %)	3.8	3.9	3.7	3.3	1.7	3.0		2.9	2.30	3.8	2.9	3.9	2.0	2.2	2.6	4.6
Gal (mol %)	35.2	30.5	48.9	42.3	43.4	37.1	50.4	42.2	44.9	49.7	46.1	47.0	34.2	40.6	36.7	32.1
Glc (mol %)			4.4		6.4	15.6		17.5	5.6	0	14.8	10.3	19.0	10.9		
uronic acid (mg/g)	148.1	165.1	172.2	127.5	129.8	117.2	79.6	131.4	196.3	89.9	162.4	127.5	63.2	55.5	265.8	175.5
protein (mg/100 mg)	5.8	6.8	5.8	6.5	5.5	7.6	6.9	6.2	6.5	7.1	9.7	6.9	6.4	2.8	2.2	5.2

[a] Samples 1−10, CSP-AGP and CST-AGP were from green tea. Samples 11 and 12 were from oolong tea. Samples 13 and 14 were from black tea.

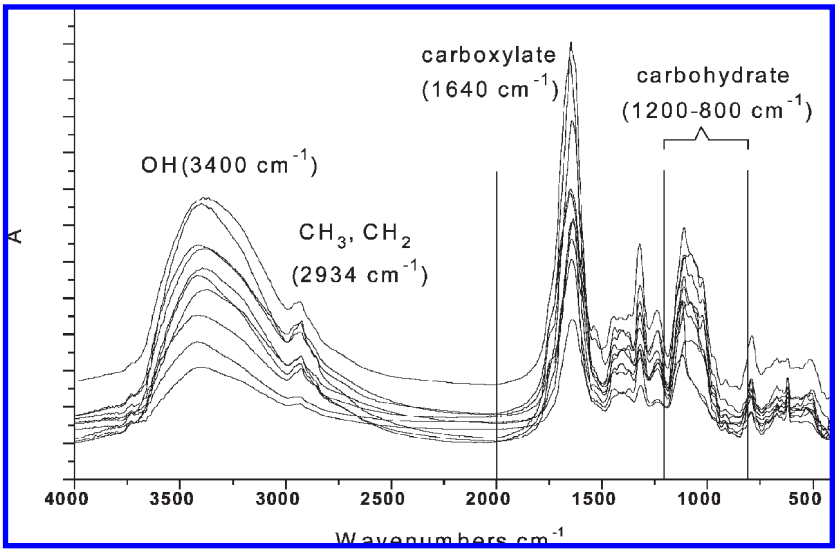

Figure 3. IR absorption spectra of green tea AGPs (sample no. 1∼10).

Statistical Analysis. SPSS 11.0 programs developed by SPSS Inc. (Chicago, IL) were used in the cluster analysis. Concretely, cos θ values of the samples were taken as variables and hierarchical cluster analysis and *K*-means cluster step were conducted.

Superoxide Radical Scavenging Activity. Superoxide radical scavenging activity was determined spectrophotometrically by monitoring the effect of tested substances on the reduction of NBT to the blue chromogen formazan by O_2^- superoxide radicals generated by the xanthine/xanthine oxidase system (X/XOD) as described previously (*20*). Briefly, 50 μL of CSW-AGP, CSP-AGP, or CST-AGP was mixed with 200 μL of mixture of 0.4 mM xanthine and 0.24 mM NBT in 0.1 M NaH_2PO_4 buffer (pH 7.8) containing 0.1 mM EDTA. A total of 50 μL of XOD (0.10 unit/mL), dissolved in the same phosphate buffer, was added, and the resulting mixture was incubated at 37 °C for 20 min. The reaction was terminated by adding 35 μL of 6% SDS solution, and the absorbance was measured at 560 nm. The superoxide scavenging activity was calculated as a percentage of NBT reduction to the formazan salt. The X/XOD system was considered to be 100% of superoxide production. Ascorbic acid was used as antioxidant standard.

Hydroxyl Scavenging Activity. The formation of $^{\bullet}OH$ (hydroxyl radical) from the Fenton reaction was quantified by determining the degradation product of 2-deoxyribose, malondialdehyde, by its condensation with 2-thiobarbituric acid (TBA) (*21*). Briefly, reactions were started by the addition of Fe^{2+} (6 μM final concentration) to solutions containing 5 mM 2-deoxyribose, 100 mM H_2O_2, and 20 mM phosphate buffer (pH 7.2). Ascorbic acid was used as antioxidant standard. Different concentrations of CSW-AGP, CSP-AGP, or CST-AGP were added to the system before Fe^{2+} was added. Reactions were carried out for 15 min at room temperature and were stopped by the addition of 4% phosphoric acid (v/v) followed by 1% TBA (w/v, in 50 mM NaOH). Solutions were boiled for 15 min at 95 °C and then cooled to room temperature. The absorbance was measured at 532 nm, and results were expressed as IC_{50}.

Ferrous Ion Chelating Ability. The ferrous ion chelating ability of the AGPs was investigated according to the method of Qi et al. (*22*). The reaction mixture containing samples (12.5−200 μg/mL), $FeCl_2$ (0.1 mL, 2 mM), and ferroizine (0.4 mL, 5 mM) were shaken well and incubated for 10 min at room temperature. The absorbance of the mixture was measured at 562 nm against a blank. The ability of all samples to chelate ferrous ion was calculated using the following equation: chelating ability (%) = (A_{562} control − A_{562} sample)/A_{562} control × 100, where A_{562} control is the absorbance of the control (distilled water, instead of sample).

RESULTS AND DISCUSSION

Selection of Second-Derivative IR and 1200−800 cm^{-1} Region. The AGP extracted from green tea was mainly composed of arabinose, galactose, and uronic acids. The protein content did not exceed 10% of the total weight (**Table 1**). IR spectra displayed the common characteristics of polysaccharides: OH at about 3400 cm^{-1}, CH_3 or CH_2 at about 2934 cm^{-1}, and carbohydrate between 1200 and 800 cm^{-1} (C−OH and C−O−C at about 1110 and 1018 cm^{-1}); the common characteristics of protein are amide I band between 1720 and 1600 cm^{-1} (the strongest peak at about 1640 cm^{-1}), amide II band between 1600 and 1500 cm^{-1} (no obvious peak), and amide III band between 1450 and 1200 cm^{-1} (the strongest peak at about 1323 cm^{-1}) (**Figure 3**).

To choose a suitable kind of IR spectra to reflect the special characteristics of green tea AGP, the vectorial angle method was applied to compare the similarity of each spectrum (including IR, first-derivative IR, and second-derivative IR spectra) of the five regions (4000−400, 800−400, 1200−800, 2000−1200, and 4000−2000 cm^{-1}) of 20 samples with that of sample 1. The closer to 1 the

Table 2. Similarity of the IR, First-Derivative IR, and Second-Derivative IR Spectra of Samples 2−21 Compared with Sample 1, Which Were Calculated by the Vectorial Angle Method[a]

	cos θ value																				
wavenumber region	1	2	3	4	5	6	7	8	9	10	11	12	13	14	15	16	17	18	19	20	21
4000−400 cm^{-1}																					
IR	1.00	0.98	0.98	0.96	0.98	0.97	0.99	0.95	0.97	0.99	0.99	0.97	0.96	0.96	0.97	0.97	0.96	0.90	0.80	0.89	0.93
first-derivative IR	1.00	0.96	0.87	0.25	0.93	0.89	0.88	0.75	0.90	0.93	0.88	0.75	0.62	0.63	0.80	0.71	0.54	0.05	0.23	0.12	0.41
second-derivative IR	1.00	0.69	0.44	0.03	0.65	0.65	0.74	0.51	0.53	0.68	0.82	0.72	0.45	0.22	0.73	0.63	0.30	−0.05	0.10	−0.04	0.38
800−400 cm^{-1}																					
IR	1.00	0.98	0.96	0.94	0.97	0.97	0.99	0.97	0.96	0.99	0.98	0.97	0.95	0.95	0.97	0.97	0.96	0.95	0.93	0.92	0.91
first-derivative IR	1.00	0.89	0.38	0.15	0.94	0.94	0.77	0.66	0.67	0.82	0.90	0.88	0.44	0.26	0.83	0.76	0.17	0.04	−0.04	−0.04	0.35
second-derivative IR	1.00	0.83	0.23	0.00	0.91	0.94	0.76	0.60	0.65	0.59	0.91	0.92	0.48	0.15	0.86	0.68	−0.07	−0.04	−0.20	−0.05	0.35
1200−800 cm^{-1}																					
IR	1.00	0.99	0.99	0.97	0.99	0.97	0.99	0.94	0.97	1.00	0.98	0.94	0.97	0.97	0.95	0.98	0.97	0.95	0.90	0.93	0.96
first-derivative IR	1.00	0.99	0.88	0.89	0.92	0.84	0.92	0.65	0.91	0.98	0.84	0.67	0.77	0.63	0.78	0.61	0.36	0.38	0.34	0.41	0.38
second-derivative IR	1.00	0.97	0.88	0.83	0.83	0.63	0.82	0.38	0.91	0.96	0.67	0.36	0.56	0.31	0.51	0.38	0.10	0.31	0.30	0.20	−0.13
2000−1200 cm^{-1}																					
IR	1.00	0.98	0.98	0.98	0.99	0.99	0.99	0.97	0.98	0.99	0.99	0.99	0.97	0.97	0.98	0.96	0.94	0.96	0.65	0.88	0.90
first-derivative IR	1.00	0.94	0.93	0.23	0.95	0.92	0.93	0.83	0.95	0.95	0.91	0.88	0.84	0.68	0.84	0.72	0.60	0.79	0.08	0.49	0.40
second-derivative IR	1.00	0.94	0.82	0.00	0.87	0.84	0.79	0.67	0.91	0.68	0.83	0.79	0.73	0.25	0.66	0.64	0.51	0.49	−0.23	0.13	0.42
4000−2000 cm^{-1}																					
IR	1.00	0.98	0.98	0.96	0.98	0.97	1.00	0.97	0.97	1.00	1.00	0.99	0.97	0.96	0.99	1.00	0.98	0.98	0.90	0.98	0.97
first-derivative IR	1.00	0.98	0.96	0.91	0.97	0.96	0.98	0.97	0.97	0.96	0.98	0.91	0.94	0.92	0.93	0.92	0.93	0.03	0.37	0.08	0.78
second-derivative IR	1.00	0.46	0.29	0.22	0.39	0.47	0.88	0.42	0.42	0.74	0.98	0.91	0.53	0.31	0.95	0.96	0.94	−0.16	−0.21	−0.16	0.82

[a] 1−21 represent samples 1−21. (1−10 were from green tea, 11 and 12 were from oolong tea, and 13 and 14 were from black tea. 15−18 were commercial TPS. 19, 20, and 21 were glucose, dextran, and chitosan, respectively.) Sample 1 was chosen as standard in the comparison. Similarity between two samples was expressed as cos θ value.

value of cos θ is, the more similar are the spectrum and the standard spectrum. The results indicated that IR could discriminate neither the green tea AGP from that of oolong tea or black tea nor the green tea AGP from monosaccharide or other polysaccharides because the cos θ values were almost above 0.90 with no apparent difference. However, in contrast, cos θ values of the first- and second-derivative IR could distinguish them fairly well (**Table 2**) because of their higher sensitivity than IR. Because the direction of the second-derivative IR absorption spectra is contrary to that of IR absorption spectra, the second-derivative data (which are multiplied by −1) can be used to observe the absorption of IR peaks conveniently. Therefore, the second-derivative IR spectra were utilized in the rapid evaluation of green tea AGP quality. Although the whole region of 4000−400 cm^{-1} was reflecting the whole characteristics of AGP extract of the green tea, there was still too much redundant information included in it that might interfere with the acquisition of essential information reflecting green tea AGPs.

To explore which region can better reflect the characteristics of green tea AGP, the whole region of 4000−400 cm^{-1} was divided into four subregions (800−400, 1200−800, 2000−1200, and 4000−2000 cm^{-1}) in analysis, and cos θ values in each subregion of samples 2−21 were calculated by comparison with sample 1. Subsequently, these cos θ values were used in the cluster analysis of samples 1−10 of green tea AGPs with samples 11−14 of oolong and black tea AGP, samples 15−18 of commercial tea polysaccharides, and samples 19−21 of other saccharides (glucose, dextran, chitosan). The hierarchical cluster analysis among five regions revealed that the 1200−800 cm^{-1} region was the most representative region (**Figure 4**). The hierarchical cluster analysis and *K*-means cluster among the 21 samples tested indicated that cos θ values in the 1200−800 cm^{-1} region could well distinguish green tea AGP from other samples into different clusters (data not shown). This region was the better choice because it more sensitively reflected the characteristics of green tea AGP. In fact, the 1200−800 cm^{-1} region is exactly the carbohydrate region that is often used in investigations of polysaccharides that commonly occur in higher plant cell walls, because each particular polysaccharide has a specific band maximum in that region (*23*).

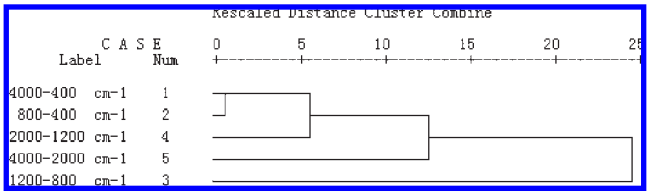

Figure 4. IR region dendrogram from hierarchical cluster analysis.

Conservative and Variable Subregions in the 1200−800 cm^{-1} Region of Second-Derivative Spectra of Green Tea AGPs. In FT-IR spectra and second-derivative IR spectra, green tea AGPs were well characterized by two bands, one being at about 1075 cm^{-1} and the other one at about 1045 cm^{-1} (**Figure 5**). Both of them are particular to β-arabinogalactans. These two bands of 1075 and 1045 cm^{-1} were shown to belong to galactopyranose in the backbone and arabinofuranose units in side branches, respectively (*24*).

In second-derivative IR spectra the 1200−800 cm^{-1} spectral region revealed several other absorption bands at about 1150, 1110, 1018, 960, 914, and 830 cm^{-1} (**Figure 5B**). Among these peaks, the two peaks at 1110 and 1018 cm^{-1} belong to uronic acids in pectic polysaccharides (*25*). Both of these two peaks appeared in the FT-IR spectra and second-derivative IR spectra, but more clearly in the latter (**Figure 5**). On the whole, the 1200−800 cm^{-1} region of second-derivative IR spectra gathered best the characteristics of the main components of green tea AGPs.

To determine the conservative subregions within this fingerprint region of green tea AGPs, the 1200−800 cm^{-1} region of second-derivative IR spectra was divided into 10 subregions, that is subregions I−X, according to the positions where absorption peaks appeared (**Figure 5B**). The similarity of second-derivative IR spectra (1200−800 cm^{-1}) of samples 2−10 compared with that of sample 1 is shown in **Table 3**. It was concluded that subregion IV (1061−1035 cm^{-1}) was the most conservative,

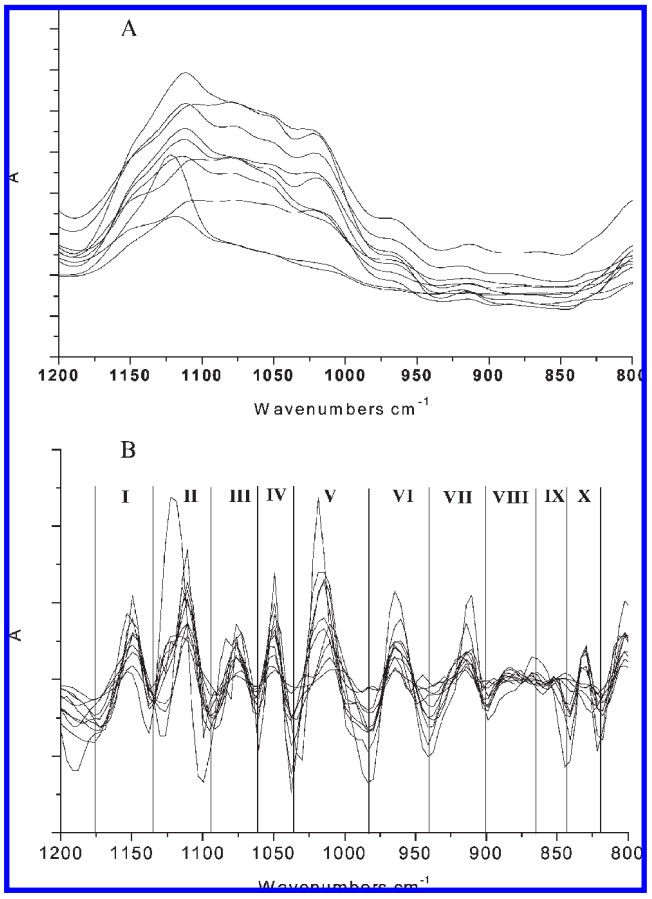

Figure 5. FT-IR (**A**) and second-derivative IR (**B**) spectra in the 1200−800 cm^{-1} region for green tea AGPs (samples 1−10). Second-derivative data were obtained by multiplying FT-IR data by −1. I, 1176−1134 cm^{-1}; II, 1134−1094 cm^{-1}; III, 1094−1061 cm^{-1}; IV, 1061−1035 cm^{-1}; V, 1035−983 cm^{-1}; VI, 983−940 cm^{-1}; VII, 940−900 cm^{-1}; VIII, 900−865 cm^{-1}; IX, 865−843 cm^{-1}; X, 843−819 cm^{-1}.

second subregions I (1176−1134 cm^{-1}), III (1094−1061 cm^{-1}), and V (1035−983 cm^{-1}), and third subregions VI (983−940 cm^{-1}) and VII (940−900 cm^{-1}); subregions II (1134−1094 cm^{-1}) and X (843−819 cm^{-1}) were somewhat variable within the sample, and subregions VIII (900−865 cm^{-1}) and IX (865−843 cm^{-1}) were the most variable subregions. These results pointed out which subregions were conservative and which ones were variable.

Quality Evaluation of Green Tea AGPs from Different Treatments by Second-Derivative IR Spectra (1200−800 cm^{-1}) and the Vectorial Angle Method. *CSW-AGP (Sample 1), CSP-AGP, and CST-AGP Extracted from Green Tea by Three Treatments.* The HPGPC results indicated that the three purified AGPs were of relative homogeneity and that the molecular mass was for all three about 40 kDa. The AGPs were mainly composed of arabinose and galactose with little proportion of rhamnose and xylose. CSP-AGP, CSW-AGP (i.e., sample 1), and CST-AGP had various degrees of substitution (A/G: 1.37, 1.57, and 1.82, respectively). Uronic acid content of CSP-AGP was the highest among the three AGPs, and that of CSW-AGP was the lowest. Amino acid analysis revealved that the three AGPs contained 17 common amino acids. The protein content of CSP-AGP was the lowest, and that of CSW-AGP was the highest (**Table 1**).

IR and Second-Derivative IR Spectra Characteristics of CSW-AGP, CSP-AGP, and CST-AGP. In FT-IR spectra, CSW-AGP, CSP-AGP, and CST-AGP were prominently characterized by two bands at about 1075 and 1045 cm^{-1} (**Figure 6A**).

Table 3. Similarity of Second-Derivative IR Spectra (1200−800 cm^{-1}) of Samples 2−10 Compared to Sample 1

	cos θ value										
sample	I	II	III	IV	V	VI	VII	VIII	IX	X	1200−800 cm^{-1}
1	1.00	1.00	1.00	1.00	1.00	1.00	1.00	1.00	1.00	1.00	1.00
2	0.97	0.99	0.96	1.00	1.00	1.00	0.94	0.91	0.95	0.98	0.97
3	0.87	0.76	0.86	0.98	0.97	0.99	0.77	−0.77	0.75	0.92	0.88
4	0.96	0.79	0.66	0.80	0.92	0.98	0.72	−0.80	0.73	0.90	0.83
5	0.97	0.93	0.90	0.91	0.78	0.52	0.96	0.73	0.22	0.47	0.83
6	0.93	0.84	0.88	0.88	0.60	−0.19	0.79	0.79	−0.58	0.08	0.63
7	0.96	0.96	0.84	0.93	0.73	0.75	0.93	0.55	0.13	0.02	0.82
8	0.49	0.52	0.74	0.97	0.94	0.85	0.85	−0.18	0.52	0.36	0.38
9	0.93	0.72	0.82	0.99	0.98	1.00	0.90	−0.84	0.94	0.87	0.91
10	0.96	0.95	0.82	0.98	1.00	0.99	0.93	0.17	0.97	0.92	0.96

Table 4. Similarity of Second-Derivative IR Spectra (1200−800 cm^{-1}) of CSP-AGP and CST-AGP Compared with CSW-AGP

	cos θ value										
sample	I	II	III	IV	V	VI	VII	VIII	IX	X	1200−800 cm^{-1}
CSP-AGP	0.82	0.37	0.97	0.94	0.92	0.91	0.95	0.15	0.59	0.58	0.77
CST-AGP	0.96	0.67	0.96	0.97	0.95	0.99	0.93	0.86	0.99	0.95	0.91

All three AGPs also revealed the same maxima around 1020 cm^{-1} and a shoulder at 964 cm^{-1}, which were both shown by Robert et al. as characteristics for an arabinogalactan (*23*).

A sensitive examination of the spectra of the three AGPs was further carried out using second-derivative spectral data (**Figure 6B**). The 1200−800 cm^{-1} spectral region revealed several absorption bands at about 1150, 1110, 1075, 1045, 1018, and 960 cm^{-1}, with their intensities increasing as the degree of substitution decreased (A/G: 1.82, 1.57, and 1.37). The glycosidic linkage ν (C—O—C) contribution dominated in the IR bands at about 1160−30 cm^{-1}. Galactose units with any link type and position were found at about 1155 cm^{-1}, at lower frequencies in polysaccharides containing arabinose, rhamnose, and mannose (*24*), and at 1150 cm^{-1} specific for the CSW-AGP, CSP-AGP, and CST-AGP. The variation of the absorption intensity at 1150 cm^{-1} of the three AGPs appears therefore to be due to the steric interaction between the arabinose side chain and the galactose backbone.

The 1200−800 cm^{-1} regions were also divided into 10 subregions according to the peaks in the second-derivative spectra of the three AGPs as previously described. The spectra similarity of CSP-AGP or CST-AGP in the 10 subregions and the whole region of 1200−800 cm^{-1} was compared with that of CSW-AGP and represented by the cos θ values. It was found that cos θ values in regions III (1090−1061 cm^{-1}), IV (1061−1037 cm^{-1}), V (1037−993 cm^{-1}), VI (993−939 cm^{-1}), and VII (939−901 cm^{-1}) between CSP-AGP or CST-AGP and CSW-AGP were more than 0.90, indicating a higher degree of similarity of the three AGPs in these regions. Similarity of the three AGPs in regions II (1125−1090 cm^{-1}) and VIII (901−864 cm^{-1}) was relatively low. Contrary to CST-AGP, the IX (864−841 cm^{-1}) and X (841−818 cm^{-1}) regions of CSP-AGP varied greatly from those of CSW-AGP as the cos θ values were only 0.59 and 0.58 in these two subregions, respectively. This similarity of these subregions was very consistent with the results obtained before. The cos θ value of the whole region of 1200−800 cm^{-1} of CST-AGP was 0.91 and that of CSP-AGP, 0.77 (**Table 4**). Generally, CST-AGP was closer to CSW-AGP than CSP-AGP in second-derivative IR spectra as well as in its composition (**Table 1**). X-ray and

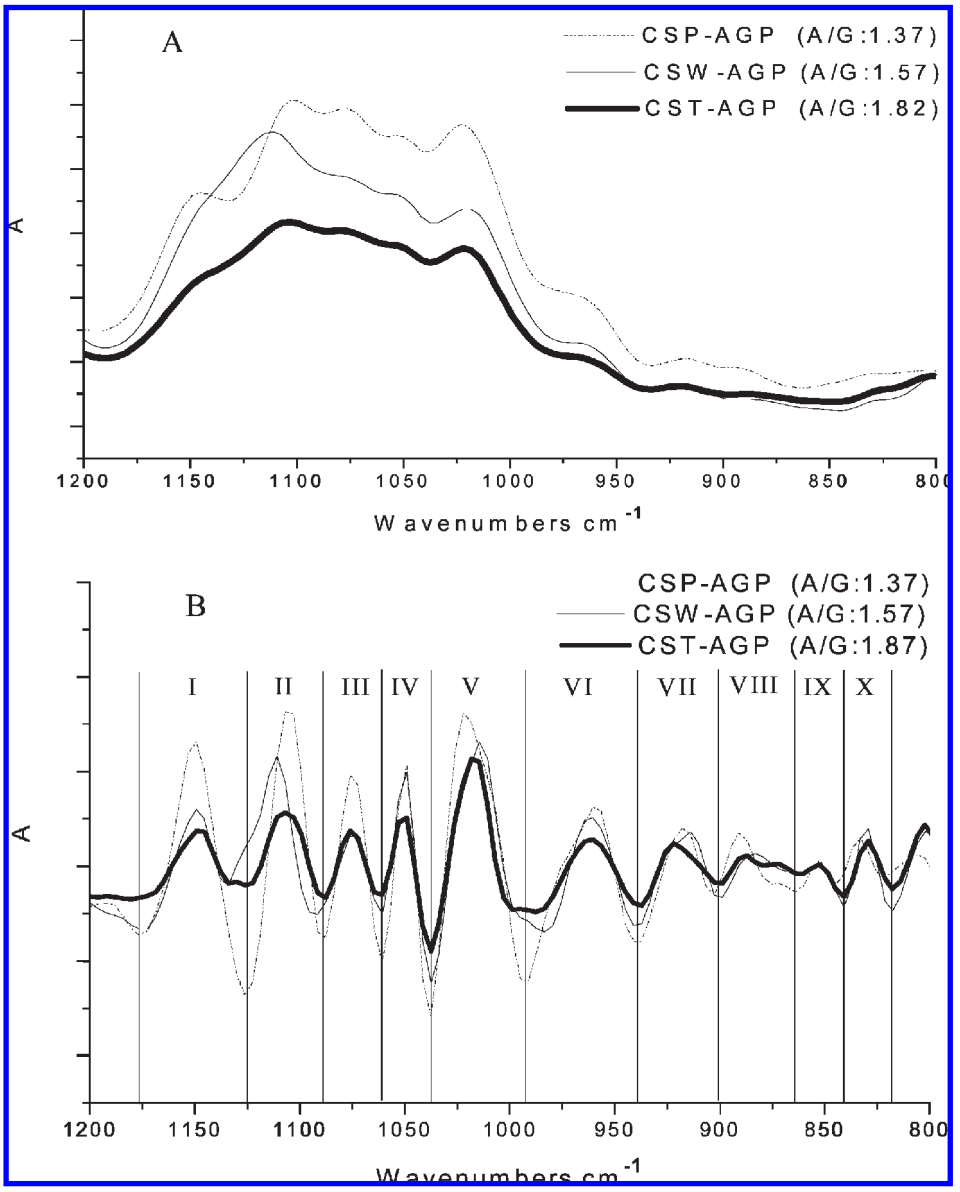

Figure 6. FT-IR spectra (**A**) and second-derivative IR spectra (**B**) in the 1200−800 cm^{-1} region for CSW-AGP, CSP-AGP, and CST-AGP. Second-derivative data are multiplied by −1. I, 1176−1125 cm^{-1}; II, 1125−1090 cm^{-1}; III, 1090−1061 cm^{-1}; IV, 1061−1037 cm^{-1}; V, 1037−993 cm^{-1}; VI, 993−939 cm^{-1}; VII, 939−901 cm^{-1}; VIII, 901−864 cm^{-1}; IX, 864−841 cm^{-1}; X, 841−818 cm^{-1}.

differential scanning calorimetry (DSC) analysis (data not shown) both also indicated that CST-AGP and CSW-AGP were more similar as suggested by the results of second-derivative IR spectra.

It could be speculated that regions III−VII (including the 1075 and 1045 cm^{-1} regions) reflected the common characteristics of green tea AGPs and that regions II, VIII, IX, and X represented more the variability in the composition and conformation of the AGPs. In summary, subtle variations in intensity and position arising from the differences in conformation and the interaction of the chemical groups were demonstrated to be a reflection of the second-derivative spectra of AGPs.

In Vitro Antioxidant Activities of CSW-AGP, CSP-AGP, and CST-AGP. To determine whether the CST-AGP was more similar in bioactivity with CSW-AGP than CSP-AGP, their in vitro antioxidant activities were investigated. Although superoxide itself is a relatively weak oxidant, it is a precursor of stronger oxidant species such as oxygen and hydroxyl radicals and can initiate lipid oxidation indirectly. CSP-AGP, the IC_{50} value of which was 261.28 μg/mL, exhibited the highest capability of scavenging superoxide among the three AGPs, followed by CSW-AGP (326.73 μg/mL) and CST-AGP (446.64 μg/mL). On the other hand, CSP-AGP had the lowest capability of scavenging hydroxyl radicals. The IC_{50} value of CSP-AGP was 395.54 μg/mL, which was much higher than that of CSW-AGP (32.38 μg/mL) or CST-AGP (82.27 μg/mL) (**Table 5**). Two types of antioxidation mechanisms were proposed for hydroxyl radicals, one by suppressing the generation of the hydroxyl radicals and the other by scavenging the hydroxyl radicals generated. In the first mechanism, the antioxidant may chelate the metal ions to form metal complexes, which cannot react with H_2O_2 to provide the hydroxyl radicals and thus suppress the generation (*26*).

Table 5. IC_{50} Values of CSW-AGP, CSP-AGP, and CST-AGP for Scavenging Superoxide and Hydroxyl Radicals (n = 3, Mean ± SD)

sample	IC_{50} O_2^- (μg/mL)	IC_{50} $^{\bullet}OH$ (μg/mL)
CSW-AGP	326.73 ± 20.3	32.38 ± 4.7
CSP-AGP	261.28 ± 19.7	395.54 ± 30.8
CST-AGP	446.64 ± 33.5	82.27 ± 5.6
ascorbic acid	127.32 ± 8.9	175.32 ± 11.3

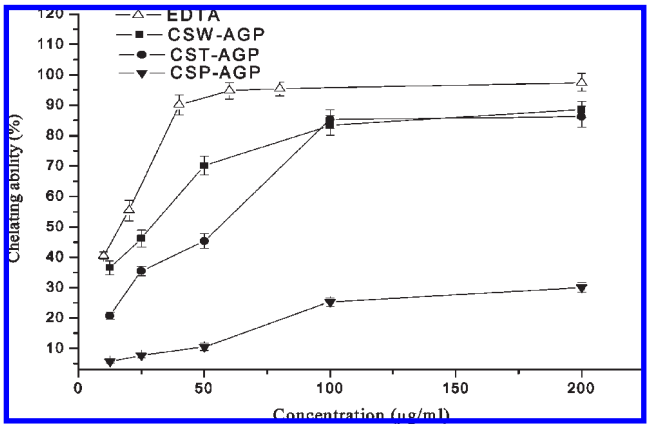

Figure 7. Chelating ability of CSW-AGP, CSP-AGP, CST-AGP, and EDTA (n = 3, mean ± SD).

Tea has been reported to have a strong ability to chelate metal ions including iron, calcium, lead, aluminum, and zinc (*27*−*29*). The polysaccharides extracted from green tea were also shown to have a strong ability to chelate iron and magnesium ions in our investigation (data not shown). The data shown here indicate that CSP-AGP had a weaker ability of chelating ferrous ion than CSW-AGP and CST-AGP. Within the concentration range of 12.5−200 μg/mL, the chelating ability ranged from 36 to 89% for CSW-AGP and from 21 to 86% for CST-AGP, but only from 6 to 30% for CSP-AGP. Compared to EDTA, the chelating abilities of CSW-AGP and CST-AGP were not much weaker (**Figure 7**). It seemed that the hydroxyl radical scavenging capabilities of CSW-AGP and CST-AGP were more likely to be attributed to their chelating abilities. Among the three AGPs, the ratio of A/G and the chelating ability of CSP-AGP were both the lowest, indicating that the chelating ability or radical scavenging ability of green tea AGPs was closely related to the structure of their arabinose side chain. In other words, it indicated that the more similar the second-derivative IR spectra of green tea AGPs were, the closer the iron chelating ability the green tea AGPs would be, so as to exhibit a similar antioxidation capability for hydroxyl radicals. The arabinogalactan is a helix-forming polymer molecule composed of a rigid core decorated with a series of flexible side groups having many hydroxyl groups that can always be exploited as drug delivery and related functions (*30*). The side groups perform dual roles in the arabinogalactan molecule: first, they shield the galactan triple helix from external turbulences so that the central core stays strong; second, they interact with neighboring helices via hydrogen bonds. The observed decrease of the superoxide radical and hydroxyl scavenging activity as well as ferrous ion chelation activity of CSP-AGP compared with those of CSW-AGP and CST-AGP may be due to the side groups in CSP-AGP having been destroyed to some degree by the pectinase so that the related activities varied.

FT-IR is one of the most widely used methods to identify chemical constituents and to elucidate their structures, and it has been extensively used to identify medicines in Pharmacopoeia of many countries owing to its fingerprint, nondestructive, and repeatable methodology (*31*). In this study, a combination of second-derivative IR analysis and the vectorial angle method was demonstrated to be an effective tool to differentiate the AGPs obtained from the green tea by different extraction treatments. Generally, the closer to 1 the value of cos θ is, the more similar are the spectrum and the standard spectrum; the more similar to the standard sample is the second-derivative IR of the test sample, the more alike their composition and bioactivities will be.

Taken together, the results indicated that the 1200−800 cm^{-1} region in the second-derivative IR spectra represents the main characteristics of green tea AGPs. Two characteristic bands at 1075 and 1045 cm^{-1}, reflecting galactopyranose in the backbone and arabinofuranose units in side branches, respectively, were identified in the IR spectra and second-derivative IR. The bands of 1110 and 1018 cm^{-1} belong to uronic acids in green tea AGPs.

This study allowed the definition of the conservative and variable subregions between 1200 and 800 cm^{-1}, which is useful for controlling the quality of green tea AGPs. The conservative region, which reflects the common characteristics of green tea AGPs, in second-derivative IR spectra lies in the 1090−900 cm^{-1} range. The variable region exists at about 1134−1094 and 900−819 cm^{-1}. According to these observations, a product of green tea AGPs should remain relatively consistent with the determined standard of green tea AGP, but might vary because of differences in the raw material, process conditions, purity, and other factors.

In summary, the method proposed in this study appears to be effective and sensitive for the distinction of green tea AGPs from other macromolecules that have a similar composition with green tea AGPs (black tea and oolong tea AGPs) or that are composed of complex components including green tea AGPs (commercial crude tea polysaccharides) or that are totally different in the component and structure with green tea AGPs (dextran and chitosan) and for the discrimination of green tea AGPs that have a different degrees of substitution. This method is useful and convenient for monitoring the compositional change in the green tea AGPs that originate from different processes. This fingerprinting approach will potentially play an important role in the fast discrimination of green tea AGPs and their quality control.

ABBREVIATIONS USED. AGP, Arabinogalactan proteins; CSW-AGP, water-extracted *Camellia sinensis* AGP; CSP-AGP, pectinase-extracted *Camellia sinensis* AGP; CST-AGP, trypsin-extracted *Camellia sinensis* AGP; HPGPC, high-performance gel permeation chromatography.

LITERATURE CITED

(1) Yamada, H.; Kiyohara, H. Complement-activating polysaccharides from medicinal herbs. *Immunomodulatory Agents from Plants*; Wagner, H., Ed.; Birkhäuser: Basel, Switzerland, 1999; Vol.*1*, pp 61−202.

(2) Yu, K. W.; Kiyohara, H.; Matsumoto, T.; Yang, H. C.; Yamada, H. Intestinal immune system modulating polysaccharides from rhizomes of *Atractylodes lancea*. *Planta Med*. **1998**, *64*, 714–719.

(3) Kiyohara, H.; Matsumoto, T.; Yamada, H. Intestinal immune system modulating polysaccharides in a Japanese herbal (Kampo) medicine, Juzen-Taiho-To. *Phytomedicine* **2002**, *9*, 614–624.

(4) Currier, N. L.; Lejtenyi, D.; Miller, S. C. Effect over time of in-vivo administration of the polysaccharide arabinogalactan on immune and hemopoietic cell lineages in murine spleen and bone marrow. *Phytomedicine* **2003**, *10*, 145–153.

(5) Classen, B.; Thude, S.; Blaschek, W.; Wack, M.; Bodinet, C. Immunomodulatory effects of arabinogalactan-proteins from *Baptisia* and *Echinacea*. *Phytomedicine* **2006**, *13*, 688–694.

(6) Cipriani, T. R.; Mellinger, C. G.; de Souza, L. M.; Baggio, C. H.; Freitas, C. S.; Marques, M. C.; Gorin, P. A.; Sassaki, G. L.; Iacomini, M. A polysaccharide from a tea (infusion) of *Maytenus ilicifolia* leaves with anti-ulcer protective effects. *J. Nat. Prod.* **2006**, *69*, 1018–1021.

(7) Burgalassi, S.; Nicosia, N.; Monti, D.; Falcone, G.; Boldrini, E.; Chetoni, P. Larch arabinogalactan for dry eye protection and treatment of corneal lesions: investigations in rabbits. *J. Ocul. Pharmacol. Ther*. **2007**, *23*, 541–550.

(8) Showalter, A. M. Arabinogalactan-proteins: structure, expression and function. *Cell. Mol. Life Sci.* **2001**, *58*, 1399–1417.
(9) Oh, S. Y.; Yoo, D. I.; Shin, Y.; Kim, H. C.; Kim, H. Y.; Chung, Y. S.; Park, W. H.; Youk, J. H. Crystalline structure analysis of cellulose treated with sodium hydroxide and carbon dioxide by means of X-ray diffraction and FT-IR spectroscopy. *Carbohydr. Res.* **2005**, *340*, 2376–2391.
(10) Quéméner, B.; Bertrand, D.; Marty, I.; Causse, M.; Lahaye, M. Fast data preprocessing for chromatographic fingerprints of tomato cell wall polysaccharides using chemometric methods. *J. Chromatogr., A* **2007**, *1141*, 41–49.
(11) Barron, C.; Robert, P.; Guillon, F.; Saulnier, L.; Rouau, X. Structural heterogeneity of wheat arabinoxylans revealed by Raman spectroscopy. *Carbohydr. Res.* **2006**, *341*, 1186–1191.
(12) Di, X.; Chan, K. K.; Leung, H. W.; Huie, C. W. Fingerprint profiling of acid hydrolyzates of polysaccharides extracted from the fruiting bodies and spores of Lingzhi by high-performance thin-layer chromatography. *J. Chromatogr., A* **2003**, *1018*, 85–95.
(13) Zhou, X. L.; Wang, D. F.; Sun, P. N.; Bucheli, P.; Li, L.; Hou, Y. F.; Wang, J. F. Effects of soluble tea polysaccharides on hyperglycemia in alloxan-diabetic mice. *J. Agric. Food Chem.* **2007**, *55*, 5523–5528.
(14) Endwin, P.; Crowell, P.; Burnett, P. Determination of the carbohydrate composition of wood pulps by gas chromatography of the alditol acetates. *Anal. Chem.* **1967**, *39*, 121–124.
(15) Blumenkrantz, N.; Asboe-Hansen, G. New method for quantitative determination of uronic acids. *Anal. Biochem.* **1973**, *54*, 484–489.
(16) Bradford, M. A. Rapid and sensitive method for the quantitation of microgram quantities of protein utilizing the principle of protein-dye binding. *Anal. Biochem.* **1976**, *72*, 248–254.
(17) Wang, L. X.; Xiao, H. B.; Liang, X. M.; Bi, K. S. Vectorial angle method for evaluating the similarity between two chromatographic fingerprints of Chinese herb. *Yao Xue Xue Bao* **2002**, *37*, 713–717.
(18) Cao, Y.; Wang, L.; Yu, X.; Ye, J. Development of the chromatographic fingerprint of herbal preparations Shuang-Huang-Lian oral liquid. *J. Pharm. Biomed. Anal.* **2006**, *41*, 845–856.
(19) Feng, Y. F.; Zhou, X.; Guo, X. L. Vectorial angle method for studying on GC fingerprint of naphtha in *Alpinia officinarum* Hance. *Zhong Yao Cai* **2006**, *29*, 10–13.
(20) Valentová, K.; Sersen, F.; Ulrichová, J. Radical scavenging and antilipoperoxidative activities of *Smallanthus sonchifolius* leaf extracts. *J. Agric. Food Chem.* **2005**, *53*, 5577–5582.
(21) Lopes, G. K. B.; Schulman, H. M.; Hermes-Lima, M. Polyphenol tannic acid inhibits hydroxyl radical formation from Fenton reaction by complexing ferrous ions. *Biochim. Biophys. Acta* **1999**, *1472*, 142–152.
(22) Qi, H.; Zhang, Q.; Zhao, T.; Hu, R.; Zhang, K.; Li, Z. In vitro antioxidant activity of acetylated and benzoylated derivatives of polysaccharide extracted from *Ulva pertusa* (*Chlorophyta*). *Bioorg. Med. Chem. Lett.* **2006**, *16*, 2441–2445.
(23) Robert, P.; Marquis, M.; Barron, C.; Guillon, F.; Saulnier, L. FT-IR investigation of cell wall polysaccharides from cereal grains. Arabinoxylan infrared assignment. *J. Agric. Food Chem.* **2005**, *53*, 7014–7018.
(24) Kačuráková, M.; Capek, P.; Sasinková, V.; Wellner, N.; Ebringerová, A. FT-IR study of plant cell wall model compounds: pectic polysaccharides and hemicelluloses. *Carbohydr. Polym.* **2000**, *43*, 195–203.
(25) Coimbra, M. A.; Barros, A.; Barros, M.; Rutledge, D. N.; Delgadillo, I. Multivariate analysis of uronic acid and neutral sugars in whole pectic samples by FT-IR spectroscopy. *Carbohydr. Polym.* **1998**, *37*, 241–248.
(26) Ueda, J.; Saito, N.; Shimazu, Y.; Ozawa, T. A comparison of scavenging abilities of antioxidants against hydroxyl radicals. *Arch. Biochem. Biophys.* **1996**, *333*, 377–384.
(27) Minamisawa, M.; Minamisawa, H.; Yoshida, S.; Takai, N. Adsorption behavior of heavy metals on biomaterials. *J. Agric. Food Chem.* **2004**, *52*, 5606–5611.
(28) Alberti, G.; Biesuz, R.; Profumo, A.; Pesavento, M. Determination of the total concentration and speciation of Al(III) in tea infusions. *J. Inorg. Biochem.* **2003**, *97*, 79–88.
(29) Amarasinghe, B. M. W. P. K.; Williams, R. A. Tea waste as a low cost adsorbent for the removal of Cu and Pb from wastewater. *Chem. Eng. J* **2007**, *132*, 299–309.
(30) Chandrasekaran, R.; Janaswamy, S. Morphology of Western larch arabinogalactan. *Carbohydr. Res.* **2002**, *337*, 2211–2222.
(31) Liu, H. X.; Sun, S. Q.; Lv, G. H.; Chan, K. K. Study on *Angelica* and its different extracts by Fourier transform infrared spectroscopy and two-dimensional correlation IR spectroscopy. *Spectrochim. Acta A: Mol. Biomol. Spectrosc.* **2006**, *64*, 321–326.

Received November 28, 2008. Revised manuscript received April 8, 2009. This work was supported by the National Nature Science Foundation of China (No. 30801241), the China Postdoctoral Science Foundation (No. 20080430854), and the Li Ka Shing Shantou University Foundation.